MODELLING BUILDING-INTEGRATED SOLAR THERMAL SYSTEMS

Christoph Maurer[1*], Christoph Cappel[1], Tilmann E. Kuhn[1]
[1]Fraunhofer Institute for Solar Energy Systems ISE, Freiburg, Germany
*corresponding author: christoph.maurer@ise.fraunhofer.de

ABSTRACT

Building-integrated solar thermal systems (BIST) outperform building-added solar thermal systems (BAST) due to smaller heat losses at the back of the collector. BIST offer economic advantages, too. The insulation behind the collector can be used to reduce the heating demand of the building as well as to increase the solar thermal yield. Therefore, less material and labour are needed. Of course, the energy flux to the building interior needs to be considered. This energy flux depends in general on the operation of the collector as well as on the irradiance. Several innovative solar thermal building skins have been modelled in detail to analyse this coupling between the active building skin and the building (Hauer, Richtfeld et al. 2012; Hauer, Richtfeld et al. 2013; Lamnatou, Mondol et al. 2015; Lamnatou, Mondol et al. in press). However, planners need an easy approach to include BIST into their calculations. Often, there is not enough budget to measure and model the new façade. This paper is based on (Maurer, Cappel et al. 2015) and presents four new models which are more accurate than completely neglecting the coupling to the building and which are less complex than detailed physical models.

INTRODUCTION

Figure 1 presents a schematic drawing of a building-added and a building-integrated solar thermal collector. Numerous models of solar thermal collectors have been presented in the past. Some of these models are suitable for building-integrated collectors (Plantier, Fraisse et al. 2003; Matuska and Sourek 2006; Hassan and Beliveau 2007; Cadafalch 2009; Maurer and Kuhn 2012), because the temperature of the building interior is included. With this type of detailed model, BIST collectors can be well characterized (Maurer 2012). However, detailed models need more calculation time than simple models and also require some effort to be adjusted to a new collector. The simplest approach is to neglect the building integration and to simulate the collector with an efficiency curve (Cooper and Dunkle 1980) as if it were building-attached and rear-ventilated. This leads to errors in the calculation of the collector gain and of the energy flux into the building. The aim of this publication is to present different modelling approaches which can be used as approximations for certain situations and which are located between the very simple and the very detailed approaches.

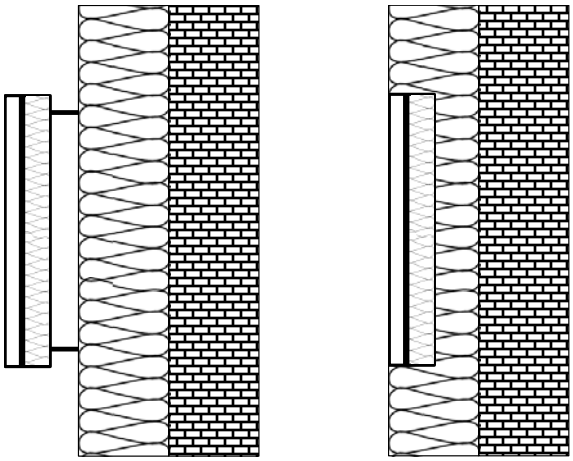

Figure 1 Schematic drawing of a building-added solar thermal collector (BAST, left-hand side) and a building-integrated solar thermal collector (BIST, right-hand side).The solar thermal absorber is indicated by a thick black line, the masonry with a brick pattern and the insulation of the wall and of the collector with insulation batting patterns.

SIMULATION MODELS

Approach A: Adaptation of the efficiency curve

If the insulation between the absorber of the BIST collector and the building interior is very thick, the heat flux and the interior may be neglected. The best solution would be to measure the efficiency curve of this collector with very good insulation of the back and the edges. If this is not possible due to financial or time restrictions and the efficiency curve is known for the BAST case, the following approach can be used to approximate the efficiency curve without back-surface losses. It is based on modifications of the BAST approach of (Cooper and Dunkle 1980).

First, the effective transmittance-absorptance product $(\tau\alpha)_e$ is calculated from the transmittance of the cover glazing τ and the absorptance of the absorber α (Duffie and Beckman 2006):

$$(\tau\alpha)_e \cong 1{,}01 * \tau * \alpha \qquad (1)$$

With this, the collector efficiency factor F' can be calculated using the efficiency for zero temperature difference between the average fluid temperature and the ambient temperature η_0:

$$F'_{BAST} = \frac{\eta_{0,BAST}}{(\tau\alpha)_e} \quad (2)$$

$(1 - F'_{BAST})$ equals the fraction of thermal losses of already absorbed energy at zero temperature difference between the average fluid temperature and the ambient temperature.

One important parameter is the fraction of thermal losses from the back surface f_{bl} which are avoided by the building integration compared to all thermal losses of a BAST collector. This fraction can be around 1/7 (Duffie and Beckman 2006). The fraction of thermal losses through the back of the collector in the BAST case is equal to $(1 - F'_{BAST}) * f_{bl}$. The fraction of additional solar thermal gain by ideal back insulation is equal to $(1 - F'_{BAST}) * f_{bl} * F'_{BIST}$. Without back-surface losses, the collector efficiency factor of the BIST case F'_{BIST} is equal to

$$F'_{BIST} = F'_{BAST} + (1 - F'_{BAST}) * f_{bl} * F'_{BIST} \quad (3)$$

and therefore

$$F'_{BIST} = F'_{BAST}/(1 - f_{bl} + f_{bl}F'_{BAST}) \quad (4)$$

The efficiency at zero temperature difference between the average fluid temperature and the ambient temperature in the BIST case $\eta_{0,BIST}$ can be calculated as:

$$\eta_{0,BIST} = (\tau\alpha)_e * F'_{BIST} \quad (5)$$

During stagnation, the mass flow and the efficiency are equal to zero. Therefore $\eta_{0,BAST}$ is equal to:

$$\eta_{0,\mathrm{BAST}} = a_{1,\mathrm{BAST}} \frac{\Delta T_{\mathrm{stag,BAST}}}{G} + a_{2,\mathrm{BAST}} \frac{(\Delta T_{\mathrm{stag,BAST}})^2}{G} \quad (6)$$

The right-hand side of this equation is equal to the thermal losses due to the stagnation temperature. In the BIST case, the fraction f_{bl} of these losses equals the BIST efficiency:

$$\eta_{\mathrm{BIST}}(\Delta T_{\mathrm{stag,BAST}}) = \eta_{0,\mathrm{BIST}} - a_{1,\mathrm{BIST}} \frac{\Delta T_{\mathrm{stag,BAST}}}{G} - a_{2,\mathrm{BIST}} \frac{(\Delta T_{\mathrm{stag,BAST}})^2}{G} = f_{\mathrm{bl}} \eta_{0,\mathrm{BAST}} . \quad (7)$$

Assuming that

$$a_{2,BIST} = a_{2,BAST} \quad (8)$$

$a_{1,BIST}$ can be fitted.

In this way, the parameters $\eta_{0,BIST}$, $a_{1,BIST}$ and $a_{2,BIST}$ of the BIST efficiency curve can be calculated from standard BAST parameters. The incidence angle modifier is the same in both cases.

If the thermal coupling between the absorber and the building interior is to be considered, the temperature of the absorber T_{abs} can be approximated by the average fluid temperature $T_{f,av}$. However, a better approximation includes the thermal resistance between the average fluid temperature and the average absorber temperature R_{fa} multiplied by the useful collector gain q_{use}:

$$T_{abs,op,BIST} = R_{fa} q_{use,BIST} + T_{f,av} \quad (9)$$

This equation also holds for the BAST case:

$$T_{abs,op,BAST} = R_{fa} q_{use,BAST} + T_{f,av} \quad (10)$$

Whenever there is no fluid flow, the stagnation temperature of the absorber T_{stag}

$$T_{abs,stag,BIST} = \Delta T_{stag,BIST} + T_a = \frac{-a_{1,BIST} + \sqrt{a_{1,BIST}^2 + 4 a_{2,BIST} G \cdot \eta_{0,BIST}}}{2 a_{2,BIST}} + T_a \quad (11)$$

can be used for the absorber temperature T_{abs}.

Within the building model, the façade collector area can be defined to be adiabatic. A more accurate approach is to link the absorber temperature with the building model to include the corresponding heat flux in the building simulation which was neglected for the calculation of the collector efficiency. Within the TRNSYS simulation environment (Beckman, Broman et al. 1994), a simple connection can be realized by estimating the thermal resistance $R_{i,BIST}$ between the absorber and the building interior and calculating the heat transfer into the building q_{int} with the temperatures of the absorber T_{abs} and the interior T_{int}:

$$q_{int} = \frac{T_{abs} - T_{int}}{R_{i,BIST}} \quad (12)$$

If an extremely well insulated wall is used within the building Type, then q_{int} can be inserted directly as additional wall gain. More advanced methods of coupling have been presented by (Hauer, Richtfeld et al. 2012; Maurer and Kuhn 2012).

Approach B: Adaptation of the collector results

Even if the heat flux between the BIST absorber and the building interior cannot be neglected, the collector may still be simulated as if it were building-attached, using some corrections to approximate the true heat flux to the interior and the increased collector gain.

First, the thermal resistance between the absorber and the interior $R_{i,BIST}$ in the BIST case needs to be calculated as well as the thermal resistance $R_{i,BAST}$ between the absorber and the air behind the back of the of the collector in the BAST case.

As in approach A, the temperature of the absorber T_{abs} can be calculated according to equations (9) and (11).

In each timestep of the simulation, the back losses of the collector can be calculated for the BAST and the BIST case:

$$q_{int,BAST} = \frac{1}{R_{i,BAST}} (T_{abs,BAST} - T_a) \quad (13)$$

$$q_{int,BIST} = \frac{1}{R_{i,BIST}} (T_{abs,BIST} - T_{int}) \quad (14)$$

with the ambient air temprature T_a and the temperature of the building interior T_{int}.

The collector gain $q_{use,BIST}$ of the BIST case can then be approximated by the collector gain $q_{use,BAST}$ and the back losses $q_{int,BAST}$ and $q_{int,BIST}$ of the two different cases:

$$q_{use,BIST} = q_{use,BAST} + q_{int,BAST} - q_{int,BIST} \quad (15)$$

Combining the equations (9), (10) (13), (14) and (15) for cases with fluid flow leads to

$$q_{use,BIST} = (q_{use,BAST} R_{i,BIST}(R_{fa} + R_{i,BAST}) + R_{i,BIST}(T_{fav} - T_a) + R_{i,BAST}(T_{int} - T_{fav})) / (R_{i,BAST}(R_{fa} + R_{i,BIST})) \quad (16)$$

As in approach A, the absorber temperature needs to be calculated by equation (11) whenever there is no fluid flow and needs to be linked to the building model to include the heat flux of the BIST area in the building simulation.

Approach C: Extended efficiency curve

An extended efficiency curve including the temperature of the building interior was proposed by (Pflug, Di Lauro et al. 2013).

There the efficiency η depends on the temperature of the ambient as well as of the building interior:

$$\eta = \eta_0 - a_{1,ext} * x - a_{2,ext} * x^2 * G - a_{1,int} * y - a_{2,int} * y^2 * G \quad (17)$$

with

- $x = \frac{T_{fav} - T_a}{G}$ [m^2*K *W^{-1}]
- $y = \frac{T_{fav} - T_{int}}{G}$ [m^2*K* W^{-1}]
- $a_{1,int}$: internal linear heat loss coefficient [W*K^{-1}*m^{-2}]
- $a_{2,int}$: internal second-order heat loss coefficient [W* K^{-2*} m^{-2}]
- $a_{1,ext}$: external linear heat loss coefficient [W*K^{-1}*m^{-2}]
- $a_{2,ext}$: external second-order heat loss coefficient [W*K^{-2}*m^{-2}]
- G: total irradiance on the collector surface [W*m^{-2}]
- $T_{fav} = \frac{a_{1,int} + T_{fo}}{2}$: the mean fluid temperature in the collector
- T_{int}: the temperature of the building interior
- T_a: the ambient temperature
- η_0: the efficiency at zero temperature difference between the fluid, the front and the back of the collector.

The assumption is that equation (17) better describes a BIST collector than the standard efficiency curve

$$\eta = \eta_0 - a_1 * x - a_2 * x^2 * G \quad (18)$$

from (Cooper and Dunkle 1980), because it includes the losses to the building interior q_{int} by

$$q_{int} = a_{1,int} * y * G + a_{2,int} * y^2 * G^2. \quad (19)$$

However, this is only true for the collector gain. The uncertainty of this approach for the heat flux to the building interior was high, e.g. equal to 48 W/m^2 in comparison to a detailed physical collector model (Pflug, Di Lauro et al. 2013).

If the thermal resistance between the absorber and the building interior is known and if the parameters $\eta_0, a_{1,ext}, a_{2,ext}, a_{1,int}$ and $a_{2,int}$ fit well to the real collector gain, then the temperature of the absorber during operation can be calculated by equation (9). For cases without fluid flow, the absorber temperature can be calculated by

$$T_{abs,stag} = \frac{1}{2(a_{2,ext}+a_{2,int})}(-a_{1,ext} - a_{1,int} + 2a_{2,ext}T_a + 2a_{2,int}T_{int} + \left((-a_{1,ext} - a_{1,int} + 2a_{2,ext}T_a + 2a_{2,int}T_{int})^2 + 4(a_{2,ext} + a_{2,int})(\eta_0 G + a_{1,ext}T_a - a_{2,ext}T_a^2 + a_{1,int}T_{int} - a_{2,int}T_{int}^2)\right)^{0.5}) \quad (20)$$

The heat flux to the interior is then better calculated by

$$q_{int} = \frac{1}{R_{i,BIST}}(T_{abs} - T_{int}) \quad (21)$$

than by equation (19).

Approach D: Simple node model

As an example of simple node models, the model presented in Figure 2 is investigated. The parallel resistance R_{ei} of this model can account for heat flux around the collector edges.

To assess this approach, the detailed physical model of (Maurer, Baumann et al. 2013) was used to calculate 2520 different cases. The following values were combined with each other: ambient temperatures of -20, 0, 20 and 40 °C, indoor temperatures of0, 10, 20, 30 and 40 °C, fluid mass flow rates of 0 and 0.02 kg/(m^{2}s), fluid inlet temperatures of 5, 15, 25, 35, 45, 55, 65, 75 and 85 °C and irradiance values of 0, 200, 400, 600, 800, 1000 and 1200 W/m^2. The cases cover most situations in a Central European climate, but are not representative in their distribution.

The thermal resistances R_e, R_i, R_{ei}, R_{fa} and the absorptance α were then varied to minimize the differences between the detailed physical model and the simple node model.

DISCUSSION

A detailed discussion was presented by (Maurer, Cappel et al. 2015). The following discussion highlights important aspects regarding the accuracy of the different approaches in typical situations and provides a comparisons between the approaches.

Neglecting the coupling

If no simple model is used and the coupling between the absorber and the building interior is neglected, then the heat flux from the building interior to the BIST element is overestimated in winter and the heat flux from the BIST element to the building interior is

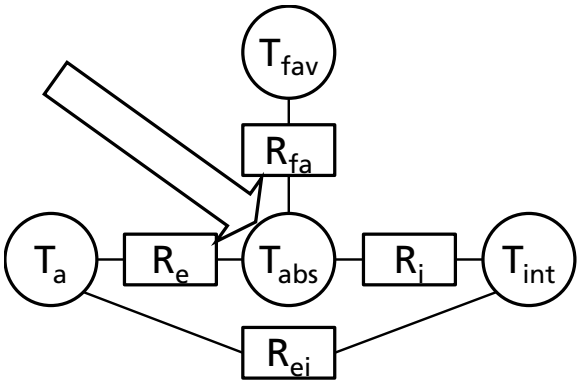

Figure 2 Schematic drawing of the simple node model., There is a parallel thermal resistance R_{ei} between the temperatures of the ambient air T_a and the building interior T_{int}. The absorber temperature T_{abs} is connected to T_a by the thermal resistance R_e and to T_{int} by the thermal resistance R_i. The absorber receives the absorbed radiation αG and is connected by the thermal resistance R_{fa} to the average fluid temperature T_{fav}.

underestimated in summer. Also, the collector gain is underestimated throughout the whole year.

If we assume a U value of 0.15 W/(m^{2}K) and a winter day with an ambient temperature of 0 °C and a room temperature of 20 °C then a calculation with a zero g value for the façade leads to heat losses of 3.1 W/m^2.

If we assume a surface temperature of the conventional façade of 3.5 °C and a BIST absorber temperature of 25 °C, then heat losses of 2.5 W/m^2 result for the conventional façade while at the BIST areas, a heat gain of 0.8 W/m^2 occurs. Without coupling, the heat losses from the BIST area are therefore overestimated by more than 3 W/m^2 in this situation.

If we assume a summer day with an ambient temperature of 30 °C, a room temperature of 25 °C, a surface temperature of the conventional façade of 45 °C and a BIST absorber temperature of 65 °C, then a pure U value calculation leads to heat gains of 0.8 W/m^2. If the temperature of the façade surface is considered, a heat flux of 3.1 W/m^2 is calculated and for the BIST areas, the heat flux amounts to 6.2 W/m^2. Without coupling, the heat gains through the BIST area are therefore underestimated by 3.1 W/m^2 in this situation.

Approach A: Adaptation of the efficiency curve

If a fraction of back losses of 1/7 is assumed, the BIST collector performance at high fluid temperatures is severely underestimated by calculating it like a BAST collector. Small errors in estimating the fraction of back losses influence the calculated BIST performance only a little.

If there is a considerable heat flux between the absorber and the building interior, the assumption of a constant fraction of back losses is not valid anymore and the temperature of the interior should be included in the calculation as presented in Approach B.

Approach B: Adaptation of the collector results

In Approach B, the temperature of the building interior is included in the calculation of the collector gain and therefore also in the calculation of the absorber temperature.

Comparing a typical BIST case with a U value of 0.24 W/(m^{2}K) with the BAST case, the stagnation temperatures in °Celsius can be 9 % higher and the collector performance 6 % higher (at an average fluid temperature of 60 °C).

Approach C: Extended efficiency curve

The accuracy of approach C depends on the accuracy of the parameters $\eta_0, a_{1,ext}, a_{2,ext}, a_{1,int}$ and $a_{2,int}$ and the thermal resistance between the absorber and the interior $R_{i,BIST}$. If $R_{i,BIST}$ is overestimated by 10%, then q_{int} is underestimated by 9%. $R_{i,BIST}$ should therefore be calculated carefully.

Approach D: Simple node model

The comparison of Approach D to a detailed model in 2520 cases lead to an estimated uncertainty of the heat flux to the interior and of the collector gain of 8%. By limiting the cases to realistic and typical situations, a higher accuracy results.

By including more parameters, the accuracy of the model can be improved as well. There is a large variety of possible, intermediate node models between this simple model and a detailed physical model.

Comparison of the Approaches

From Approach A to Approach D, the required quality of the necessary input increases. Approach A only needs the efficiency parameters of the collector datasheet. It is well suited for good insulation between the absorber and the building interior. When the heat flux between the absorber and the interior becomes relevant, Approach B is recommended. It needs a little more effort than Approach A, but still delivers accurate results without additional measurements. If measurement results are available, for instance from a demonstration installation, the efficiency curve (17) can be fitted to this data and provides a more accurate calculation of collector gain, stagnation temperature and heat flux to the interior than Approaches A and B, since it includes the influence of real integration including e.g. edge effects. Approach C is recommended in cases where e.g. monitoring data of the BIST collector performance is available. For new BIST elements, simultaneaous measurements of the collector gain and the heat flux to the interior are recommended to calibrate the simple model of Approach D. This already allows an analysis of the benefits of the new

component under various conditions. If high accuracy in certain situations is needed, the model of Approach D can be easily extended to include additional relevant physical effects.

CONCLUSION

This paper presented a variety of simple models for BIST façade elements. Depending on the available data, an approach with acceptable uncertainty can be chosen. Based on this analysis, further models can be developed to reduce the remaining uncertainties. For instance, a correction could be developed to derive the efficiency curve of vertically installed collectors from the parameters extracted from measurements on tilted collectors. In the future, a standard for models of active façade elements will be helpful to ensure the quality of a model provided to the planner.

ACKNOWLEDGEMENT

This work was funded by the German Federal Ministry for Economic Affairs and Energy, based on a decision by the German Bundestag. The authors thank the European Union for support in COST Action TU1205- BISTS and Helen Rose Wilson for proofreading this paper.

NOMENCLATURE

SYMBOL	EXPLANATION
α	Absorptance of the absorber in the collector
$a_1, a_{1,BAST}, a_{1,BIST}, a_{1,ext}, a_{1,int}$	First-order collector efficiency coefficients in general, in the BAST case, in the BIST case, for the exterior, for the interior (W/(m^{2}K))
$a_2, a_{2,BAST}, a_{2,BIST}, a_{2,ext}, a_{2,int}$	Second-order collector efficiency coefficients in general, in the BAST case, in the BIST case, for the exterior, for the interior (W/(m^{2}K^2))
BAST	Building-added solar thermal
BIST	Building-integrated solar thermal
F'	Collector efficiency factor
G	Solar irradiance (W/m^2)
$\eta, \eta_{BAST}, \eta_{BIST}, \eta_0, \eta_{0,BAST}, \eta_{0,BIST}$	Collector efficiency $\eta=\eta_0-a_1x-a_2x^2G$ in general, in the BAST case, in the BIST case, collector efficiency at x=0, in the BAST case, in the BIST case
$q_{use}, q_{use,BAST}, q_{use,BIST}$	Solar thermal collector gain in general, in the BAST case and in the BIST case (W/m^2)
q_{int}	Heat transfer from the collector to the building interior (W/m^2)
$R_e, R_{e,BAST}, R_{e,BIST}$	Thermal resistance between the absorber and the ambient temperature in general, for the BAST case, for the BIST case (m^{2}K/W)
R_{fa}	Thermal resistance between the absorber and the average fluid temperature (m^{2}K/W)
$R_i, R_{i,BAST}, R_{i,BIST}$	Thermal resistance between the absorber and the temperature of the building interior in general, for the BAST case, for the BIST case (m^{2}K/W)
τ	Transmittance of the cover of the collector
$(\tau\alpha)_e$	Effective transmittance-absorptance product
TSTC	Transparent solar thermal collector
T_a, T_{int}, T_{fav}, T_{fi}, T_{fo}, T_{abs}, $T_{abs,op}$, $T_{abs,sta}$	Temperature of the ambient air, of the building interior, of the fluid (average), of the fluid inlet, of the fluid outlet, of the absorber, of the absorber during collector operation and of the absorber during stagnation (K)
U	U value (W/(m^{2}K))
x	Difference between the average fluid temperature and the ambient temperature divided by the solar irradiance (m^{2}K/W)
y	Difference between the average fluid temperature and the temperature of the building interior divided by the solar irradiance (m^{2}K/W)

REFERENCES

Beckman, W. A., L. Broman, et al. (1994). "TRNSYS The most complete solar energy system modelling and simulation software." Renewable Energy **5**(1-4): 486-488.

Cadafalch, J. (2009). "A detailed numerical model for flat-plate solar thermal devices." Solar Energy **83**(12): 2157-2164.

Cooper, P. I. and R. V. Dunkle (1980). "A non-linear flat-plate collector model." Solar Energy **26**(2): 133-140.

Duffie, J. A. and W. A. Beckman (2006). Solar engineering of thermal processes. Hoboken N.J., Wiley.

Hassan, M. A. and Y. Beliveau (2007). "Design, construction and performance prediction of integrated solar roof collectors using finite

element analysis." Construction and Building Materials **21**(5): 1069-1078.

Hauer, M., A. Richtfeld, et al. (2013). Gebäudegekoppelte Simulation fassadenintegrierter Kollektoren mit TRNSYS. 23. OTTI-Solarthermie Symposium. Bad Staffelstein.

Hauer, M., A. Richtfeld, et al. (2012). Gekoppeltes TRNSYS-Modell zur thermischen Bewertung von Fassadenkollektoren. e-nova-Konferenz. Pinkafeld.

Lamnatou, C., J. Mondol, et al. (in press). "Modelling and simulation of building-integrated solar thermal systems: behaviour of the coupled building/system configuration." Renewable & Sustainable Energy Reviews.

Lamnatou, C., J. D. Mondol, et al. (2015). "Modelling and simulation of Building-Integrated solar thermal systems: Behaviour of the system." Renewable and Sustainable Energy Reviews **45**(0): 36-51.

Matuska, T. and B. Sourek (2006). "Façade solar collectors." Solar Energy **80**(11): 1443-1452.

Maurer, C. (2012). Theoretical and experimental analysis and optimization of semi-transparent solar thermal façade collectors. Ph.D. Dissertation, Karlsruher Institut für Technologie (KIT).

Maurer, C., T. Baumann, et al. (2013). "Heating and cooling in high-rise buildings using facade-integrated transparent solar thermal collector systems." Journal of Building Performance Simulation **6**(6): 449-457.

Maurer, C., C. Cappel, et al. (2015). "Simple models for building-integrated solar thermal systems." Energy and Buildings **103**: 118-123.

Maurer, C. and T. E. Kuhn (2012). "Variable g value of transparent façade collectors." Energy and Buildings **51**: 177-184.

Pflug, T., P. Di Lauro, et al. (2013). Evaluation of a simplified model for façade collectors. Building Simulation Conference. Chambéry, France, IBPSA.

Plantier, C., G. Fraisse, et al. (2003). Development and experimental validation of a detailed flat-plate solar collector model. ISES Solar World Congress. Göteborg, Sweden, International Solar Energy Society (ISES).